On the kinetics of isothermal crystallization of branched polyethylene

G. R. Strobl, T. Engelke, E. Maderek and G. Urban
Institut für Physikalische Chemie, Universität Mainz, Mainz, German Federal Republic
(*Received* 22 *December* 1982; *revised* 14 *March* 1983)

Isothermal crystallization of branched polyethylene was studied by time-dependent small-angle X-ray scattering experiments and dilatometry. A strict proportionality between scattering intensities and density changes was found for all times. This result indicates complete absence of crystal thickening and perfectioning processes. Isotherms directly reflect the increase in specific inner surface resulting from nucleation and lateral growth of lamellae. The shape of isotherms suggests a time-dependent non-uniform internal structure of spherulites with a decrease in specific inner surface with increasing distance from centre.

Keywords Crystallization kinetics; branched polyethylene; small-angle X-ray scattering; dilatometry

INTRODUCTION

It has been noted by several authors[1-3] that low-density polyethylene shows crystallization isotherms which cannot be explained on the basis of a simple Avrami theory[4,5]. Analysis of data starting from the Avrami equation gives values for the Avrami coefficient n which change with time and lie in the range between 1 and 2.5 rather than taking on the integral value $n=3$ or $n=4$ as would be expected for the growth of spherulites after athermal or thermal nucleation[6]. Recently we have carried out a combined dilatometric and small-angle X-ray scattering study on the kinetics which enables some straightforward conclusions on the source of this 'anomalous' behaviour. Experiments were performed on a commercial low-density polyethylene and a fraction with reduced polydispersity. The results are reported and discussed.

EXPERIMENTAL

The two polyethylene samples under examination were

I: Lupolen 1800 S, supplied by BASF AG, Ludwigshafen (methyl group concentration $33\,CH_3/1000\,C$)

II: a fraction of sample I with $M_v \approx 80000$ (the fractionation procedure which has been applied is described elsewhere[15]; the branch content is very similar to sample I).

Dilatometric measurements were carried out in a conventional mercury dilatometer[7]. It was quickly transferred from a bath kept at the temperature of the melt (120°C) to a second bath preset at the crystallization temperature. Isothermal conditions were reached in less than 2 min. The starting level of the mercury column was well defined due to the sufficiently long induction period and could in addition be fixed by linear extrapolation of the isobar from the melt region. Taking the time of transfer as zero, the level of the falling mercury column was registered as a function of time. With the knowledge of the diameter of the capillary, which had been determined before by a calibration measurement with pure mercury, specific volumes could be derived from the column height.

Small-angle X-ray scattering (SAXS) experiments were performed with a Kratky camera and Cu Kα radiation. A proportional counter with pulse-height discrimination was used as detector. Absolute intensities were obtained after having determined the primary beam intensity by a calibrated standard sample supplied by Kratky. Details which include also the procedure employed for the slit-height correction are described elsewhere[8,9]. Analysis was based on the electron-density correlation functions which were calculated by a Fourier transformation of the desmeared Lorentz factor corrected curves[10]. Samples were platelike with a thickness of 3 mm which corresponds to the optimum value[11]. This thickness is not only preferable in view of achieving maximal intensities but, more important, absolutely necessary for kinetic experiments in order to reduce intensity changes following from a possible slight change in the sample thickness to practically negligible values. Samples were melted at 120°C using a heating device within the camera, which then was quickly cooled with a stream of nitrogen to the crystallization temperature. Temperature equilibrium was established within 2 min just as for the dilatometer, so that the thermal histories were largely identical for the two experiments. In conformity with the dilatometer experiment, the start of cooling was chosen as time zero. Great care was taken to perform the dilatometric and the SAXS experiments at identical temperatures. For this purpose the platinum resistance thermoelement employed in the heating device was calibrated in the bath used for the dilatometry.

RESULTS

Crystallization kinetics

During isothermal crystallization at T_c the SAXS curve

0032-3861/83/121585-05$03.00

develops continuously. We studied the kinetics by a simple measurement of the intensity scattered in a fixed direction,

$$s = 2\sin\theta/\lambda = 2.7 \times 10^{-2}\,\mathrm{nm}^{-1}$$

(θ = Bragg angle, λ = X-ray wavelength) as a function of time. This dependence was compared to the dilatometric isotherm

$$\Delta\rho(t) = \rho(t) - \rho_a$$

(ρ_a denotes the amorphous density at T_c). *Figures 1a* and *2a* show the results of three measurements, sample I at 100°C, sample II at 100°C and 102°C. The full curves represent the time-dependent densities, the additional points give the measured scattering intensities, choosing a scale on the vertical axis to enable direct comparison. The result of the comparison is clear: there is always perfect coincidence between the two curves. Obviously $\Delta\rho(t)$ and $I(t)$ are proportional to each other over the whole time range of observations. This range includes not only the curved part of the isotherm, i.e. primary crystallization, but also the beginning of secondary crystallization, which as usual follows the law[1]:

$$\mathrm{d}\rho/\mathrm{d}(\lg t) = \text{constant}$$

In order to check if the isotherms can be described by the Avrami equation

$$\Delta\rho(t) \sim 1 - \exp(-kt^n)$$

plots of $\lg[-\ln(1-\Delta\rho/\Delta\rho(t_E))]$ versus $\lg t$ were set up (t_E denotes the time at the end of primary crystallization indicated in the figures). They are shown in *Figures 1b* and *2b*. The derivatives give Avrami coefficients in the range $n = 1$ to 1.5.

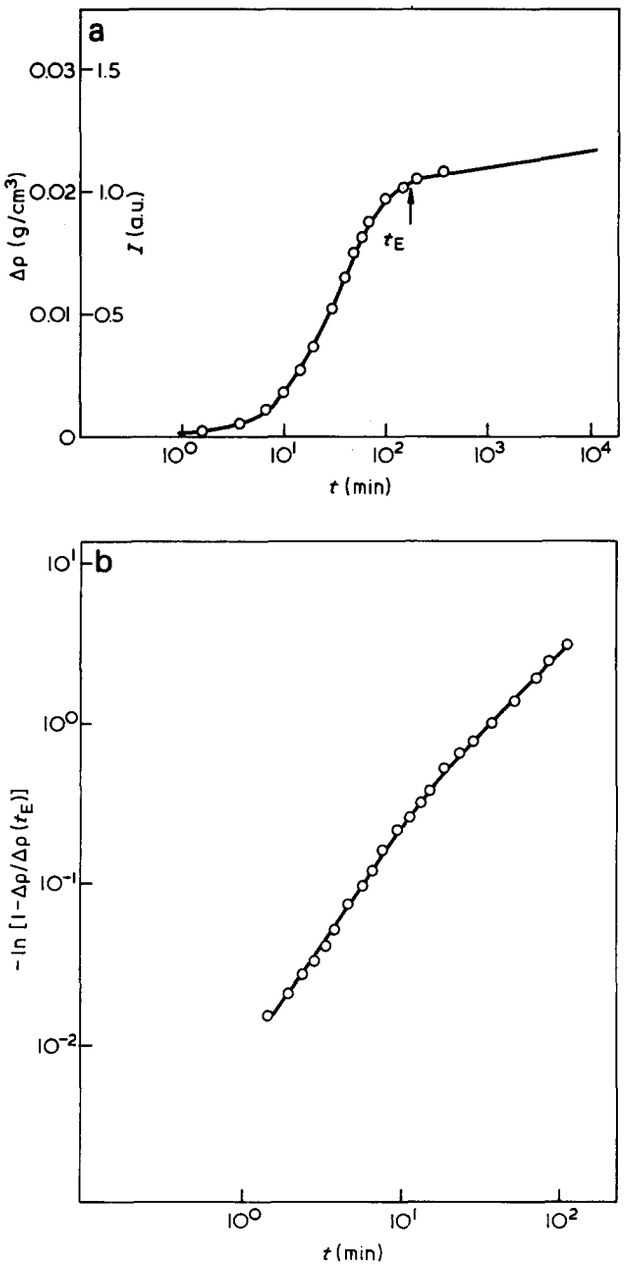

Figure 1 Isothermal crystallization of Lupolen 1800 S at 100°C. (a) Comparison of density increase $\Delta\rho(t) = \rho(t) - \rho_a$ (full curve) with SAXS intensity $I(t)$ (open circles). (b) Avrami plot of isotherm

SAXS analysis of lamellar structure

As shown by previous investigations[1,2] on sample I, the crystalline–amorphous superstructure is built up of isotropically oriented stacks of crystalline lamellae. Important parameters of the structure are the crystallite thickness d_c, the specific internal surface O_s (crystalline amorphous interface area per unit volume), the volume crystallinity $w_c = d_c O_s/2$, the long spacing L and the electron density difference $\eta_c - \eta_a$. They can be all derived from the electron-density correlation function. *Figure 3* shows in a schematic drawing the relevant properties of this function. A detailed explanation has been given elsewhere[10]. Note that the baseline coordinate A can be directly compared to the density increase measured in the dilatometer:

$$-A = w_c^2(\eta_c - \eta_a)^2 = (\rho - \rho_a)^2(\tfrac{8}{14}\,\text{mole electron/g})^2 \qquad (1)$$

Equation (1) provides a check for the consistency of the dilatometric and the SAXS measurement. *Figure 3* and equation (1) refer to a sample which is homogeneously filled with lamellar stacks, as should be the case at the end of primary crystallization. We only remark here that equation (1) becomes invalid and some of the properties indicated in *Figure 3* become modified for heterogeneous systems[10].

SAXS curves have been measured for samples I and II after 8 h of isothermal crystallization at 100°C. *Figures 4* and *5* show the desmeared and Lorentz factor corrected scattering curves $4\pi j s^2$ in absolute units and derived correlation functions. The correlation functions yield the following structure parameters:

sample I:
$d_c = 6.0\,\mathrm{nm}$
$O_s = 4.6 \times 10^{-1}\,\mathrm{nm}^{-1}$
$w_c = 0.14$

$L = 38.0\,\mathrm{nm}$
$\eta_c - \eta_a = 9.0 \times 10^{-2}$ mole electron/cm³

sample II:
$d_c = 5.7\,\mathrm{nm}$
$O_s = 7.0 \times 10^{-1}\,\mathrm{nm}^{-1}$
$w_c = 0.20$

$L = 30\,\text{nm}$
$\eta_c - \eta_a = 8.4 \times 10^{-2}$ mole electron/cm^3

The lamellar thickness d_c and the electron density differences $\eta_c - \eta_a$ of the two samples agree within the error limits of the measurement. Equation (1) turns out to be valid for both samples. The values obtained are

sample I:
$A = 0.15 \times 10^{-3}$(mole electron/cm^3)^2

$\rho(t = 480\,\text{min}) - \rho_a = 0.021$ g/cm^3

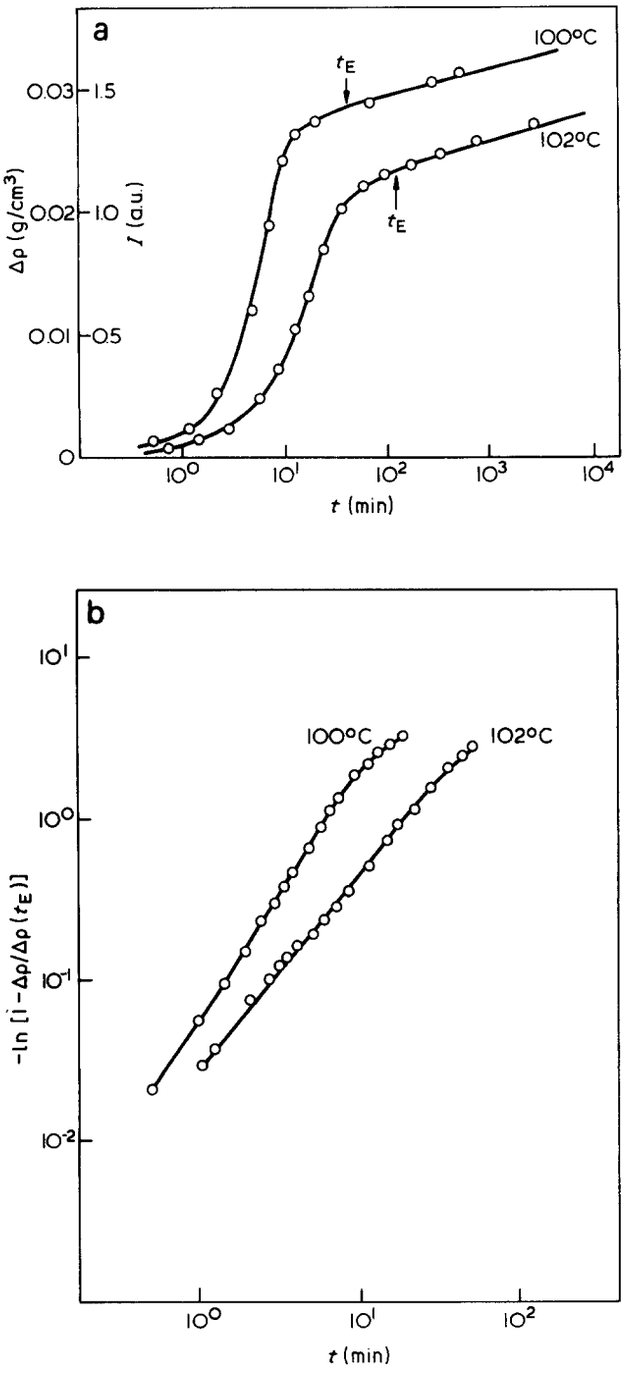

Figure 2 Isothermal crystallization of a fraction of branched polyethylene at 100° and 102°C. (a) Comparison of density increase $\rho(t) = \rho(t) - \rho_a$ (full curve) with SAXS intensity $I(t)$ (open circles). (b) Avrami plots of isotherms

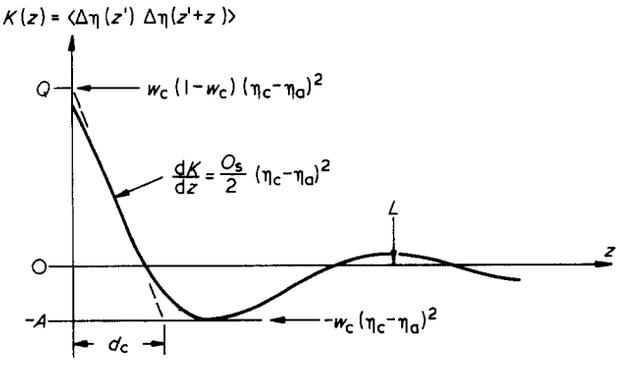

Figure 3 General shape and properties of the electron-density correlation function $K(z)$

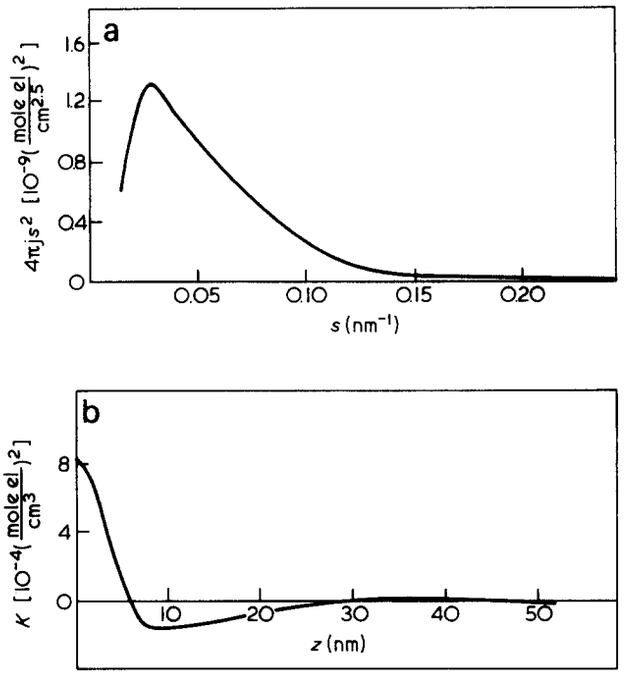

Figure 4 SAXS analysis of lamellar structure of Lupolen 1800 S after isothermal crystallization at 100°C. (a) Desmeared SAXS curve. (b) Derived electron-density correlation function

sample II:
$A = 0.30 \times 10^{-3}$(mole electron/cm^3)^2

$\rho(t = 480\ \text{min}) - \rho_a = 0.031$ g/cm^3

A check shows consistency within the error limits. From this we can be sure that the samples had a homogeneous structure at the time of the measurement. Further conformation of the homogeneity followed from a separate investigation in a polarizing microscope: samples crystallized at 100°C using a hot stage became completely filled with spherulites[13].

DISCUSSION

Our measurements confirm the peculiarity in the crystallization kinetics of low-density polyethylene reported by the other authors.

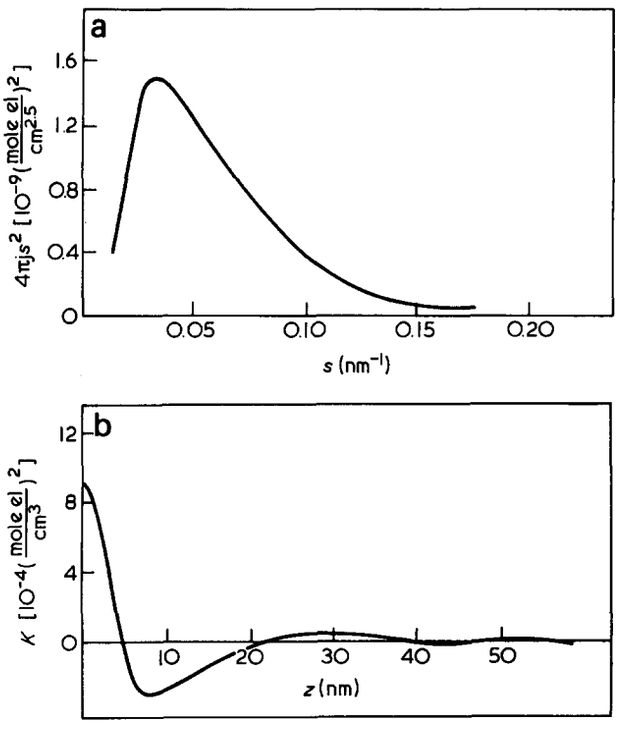

Figure 5 SAXS analysis of lamellar structure of a fraction of branched polyethylene after isothermal crystallization at 100°C. (a) Desmeared SAXS curve. (b) Derived electron-density correlation function

For an analysis of data, it is helpful to separate the density change $\Delta\rho=(\rho-\rho_a)(t)$ into several contributing factors. First it is

$$(\rho-\rho_a)(t)=\phi_s(\rho-\rho_a)_s \tag{2}$$

with ϕ_s = volume fraction occupied by spherulites and $(\rho-\rho_a)_s$ = density increase within spherulites.

Furthermore we have

$$(\rho-\rho_a)_s=w_c^s(\rho_c-\rho_a)=\frac{O_s^s}{2}d_c(\rho_c-\rho_a) \tag{3}$$

with w_c^s = crystallinity within spherulites and O_s^s = specific internal surface within spherulites.

Starting from these relations we inquire about the possible sources of the strong deviations from the Avrami theory.

A constant radial growth rate of the spherulites leads to an Avrami expression for ϕ_s:

$$\phi_s=1-\exp(-kt^n)$$

with $n=3$ or 4 for athermal or thermal primary nucleation, respectively. Segregation processes may cause a retardation of growth rates due to the accumulation of non-crystallizable sequences or low molecular weight chains in front of the growing spherulites. This effect has been observed and disucssed for random copolymers of ethylene and vinyl acetate by Nachtrab and Zachmann[14]. However, it seems unlikely to us that it can account for a change of n from 3 to 1–2, since low values are observed from the earliest stage of crystallization. Our belief is supported by the similarity in crystallization behaviours between the fraction and the polydisperse sample. The two samples certainly differ in the amount of chain segregation during crystallization[15], but there is no effect visible in the isotherms.

Hence, the factor $\phi_s(t)$ most probably cannot account for the observations. We have to conclude that $(\rho-\rho_a)_s$ is not a constant, but depends on the position within the spherulite and on time.

Principally the variation can be due to O_s^s, d_c or $(\rho_c-\rho_a)$, that means due to lateral growth of lamellae, crystal thickening or perfectioning of crystals. It is possible to discriminate between these three factors. The key is provided by the comparative $\rho(t)/I(t)$ measurements.

The SAXS intensity can be generally written as[8]:

$$js^2\sim\phi_s\frac{O_s^s}{2}(\eta_c-\eta_a)^2F^2(s)G(s) \tag{4}$$

with

$$F^2=d_c^2\frac{\sin^2\pi d_c s}{(\pi d_c s)^2}$$

being the structure factor of lamella and G the interference function.

The time-dependent intensity measurements were performed at low s-values, where F^2 can be approximated by

$$F^2=d_c^2$$

We have furthermore $(\eta_c-\eta_a)\sim(\rho_c-\rho_a)$. The slit-smearing effect can be accounted for by replacing $G(s)$ by a 'smeared' interference function $\tilde{G}(s)$. We thus arrive at the following simple expression for the measured intensity I:

$$I\sim\phi_s\frac{O_s^s}{2}(\rho_c-\rho_a)^2d_c^2\tilde{G}(s) \tag{5}$$

A comparison of equation (5) with equations (2) and (3) shows the same linear dependence of $\rho-\rho_a$ and I on the specific internal surface $O_s=\phi_sO_s^s$ but different functional dependence on $(\rho_c-\rho_a)$ and d_c, namely linear compared to quadratic ones. Considering these relations, the results given in *Figure 6* provide a clear answer: $(\rho_c-\rho_a)$ and d_c are constant during crystallization, the kinetics rely exclusively on the nucleation and growth of lamellae, i.e. on $O_s(t)$. Only under these conditions can a proportionality $I\sim(\rho-\rho_a)$, as has been observed, arise. The shape of the isotherm therefore reflects the time dependence $O_s(t)$.

The experimental result $n=1$–2 indicates that the internal specific surface O_s^s is not a constant within the spherulites. It must depend on the distance from the centre and the time, $O_s^s(r,t)$. This is in fact not surprising at all. Banks[3] pointed out that for dendritic growth there is a decrease in the density of branches with increasing distance from the centre. The reason for this behaviour is easily seen. There are two independent processes: the rate of lateral growth of existing lamellae and the rate of branching of the lamellae or nucleation of new lamellae. The second process is necessary for spherulites to end up with a homogeneous microstructure. The density within a growing spherulite will depend on the ratio of the two rates: the density is uniform only if the branching rate is sufficiently high and will drop with increasing distance from the centre if the branching rate is too low. In the extreme case of absence of any branching and one-dimensional growth of ribbon-like lamella, one has:

$$O_s^s\sim 1/r^2 \tag{6}$$

The density distribution (6) leads to an Avrami coefficient $n=1$, characteristic for the linear growth of the few existing lamellae.

Hence, the observed shape of the isotherms can be considered as indicative of a comparatively slow branching rate. The structural reason for this is open to speculation.

It came as a surprise to us that the proportionality $I(t)\sim(\rho-\rho_a)(t)$ is not only valid for the primary crystallization but extends into the long-time regime with $d\rho/d(\ln t)=$ constant. This observation shows that neither crystal perfectioning processes (increase of ρ_c) nor a crystal thickness growth (increase of d_c), both being mechanisms repeatedly discussed in the literature (ref. 6, ch. 6.1.6), contribute to secondary crystallization in low-density polyethylene. Our results suggest a very slow further lateral extension of lamellae.

The two parameters d_c and $(\rho_c-\rho_a)$ which remain constant throughout the crystallization have been determined by the SAXS analysis. With the knowledge of these values:

$$d_c=(5.8\pm0.2)\,\text{nm}$$

$$\rho_c-\rho_a=(0.152\pm0.008)\,\text{g/cm}^3$$

it is possible to derive from a dilatometric isotherm $\Delta\rho(t)$ the time-dependent crystallinity and internal specific volume:

$$w_c(t)=\Delta\rho(t)/(\rho_c-\rho_a)$$

$$O_s(t)=\frac{2\Delta\rho(t)}{(\rho_c-\rho_a)d_c}$$

We consider the constancy of d_c as being due to the branches, which hinder longitudinal chain diffusion through the crystals and therefore suppress crystal thickness growth. In this important respect, linear and branched polyethylene differ from each other. In our understanding it is exactly this difference in chain mobility which leads to the different crystallization behaviour, as reflected in the broadness of the crystallization ranges. In the model recently suggested[12], partial crystallization has been associated with variations in the branch concentration of different amorphous layers. Such variations can only occur if the transport of branches through the crystallites is blocked. The observed constancy of d_c during isothermal crystallization indicates that this is in fact the case.

ACKNOWLEDGEMENTS

Thanks are due to Dr Haberkorn, BASF AG, for supplying us with sample material. The research has been granted by the Deutsche Forschungsgemeinschaft (Sonderforschungsbereich 41 'Physics and Chemistry of Macromolecules').

REFERENCES

1 Kovacs, A. J. *Ricerce Sci.* 1955, **251**, 669
2 Buchdahl, R., Miller, R. L. and Newman, S. *J. Polym. Sci.* 1959, **36**, 215
3 Banks, W., Gordon, M., Roe, R. J. and Sharples, A. *Polymer* 1963, **4**, 61
4 Avrami, M. *J. Chem. Phys.* 1939, **7**, 1103
5 Evans, U. R. *Trans. Faraday Soc.* 1945, **41**, 365
6 Wunderlich, B. 'Macromolecular Physics', Vol. 2, Academic Press, New York, 1978
7 Bekkedahl, N. *J. Res. Nat. Bur. Stand.* 1949, **42**, 145
8 Strobl, G. R. *Koll. Z. Z. Polym.* 1972, **250**, 1039
9 Strobl, G. R. *Acta Cryst. A* 1970, **26**, 367
10 Strobl, G. R. and Schneider, M. *J. Polym. Sci., Polym. Phys. Edn.* 1980, **18**, 1343
11 Alexander, L. E. 'X-Ray Diffraction Methods in Polymer Science', Wiley, New York, 1969, p 68
12 Strobl, G. R., Schneider, M. and Voigt-Martin, I. *J. Polym. Sci., Polym. Phys. Edn.* 1980, **18**, 1361
13 Engelke, T. Diplomarbeit, Mainz, 1980
14 Nachtrab, G. and Zachmann, H. G. *Ber. Bunsenges.* 1970, **74**, 837
15 Maderek, E. and Strobl, G. R. *Colloid Polym. Sci.* 1983, **261**, 471